Graefe's Archive for Clinical and Experimental Ophthalmology (2019) 257:583–589
https://doi.org/10.1007/s00417-018-04225-7

CORNEA

In vivo confocal microscopy morphometric analysis of corneal subbasal nerve plexus in dry eye disease using newly developed fully automated system

Giuseppe Giannaccare[1] · Marco Pellegrini[1] · Stefano Sebastiani[1] · Fabiana Moscardelli[1] · Piera Versura[1] · Emilio C. Campos[1]

Received: 29 August 2018 / Revised: 7 December 2018 / Accepted: 18 December 2018 / Published online: 14 January 2019

Abstract

Purpose To evaluate in vivo confocal microscopy (IVCM) features of corneal subbasal nerve plexus (SNP) in the setting of dry eye disease (DED) using fully automated software "ACCMetrics," and to further investigate its diagnostic performance in discriminating DED patients.

Methods IVCM exams of SNP in DED patients and matched control subjects were performed using Heidelberg Retina Tomograph with the Rostock Cornea Module. The following parameters were obtained with ACCMetrics: corneal nerve fiber density (CNFD), corneal nerve branch density (CNBD), corneal nerve fiber length (CNFL), corneal nerve total branch density (CTBD), corneal nerve fiber area (CNFA), corneal nerve fiber width (CNFW), and corneal nerve fractal dimension (CNFrD). The Mann–Whitney U test was used to compare variables. Receiver operating characteristic curves with calculations of the area under the curve (AUC) were used to describe the accuracy of IVCM parameters for discriminating DED patients from controls.

Results Thirty-nine DED patients and 30 control subjects were included. Significantly, lower values of CNFD, CNBD, and CNFL and higher value of CNFW were found in DED patients compared to controls (respectively, 20.5 ± 8.7 vs 25.4 ± 6.7 n/mm^2; 25.6 ± 20.1 vs 37.6 ± 21.5 n/mm^2; 12.6 ± 4.4 vs 14.5 ± 2.9 mm/mm^2; 0.021 ± 0.001 vs 0.019 ± 0.001 mm/mm^2; always $p < 0.024$). CNFW value had the highest diagnostic power in discriminating DED patients (AUC = 0.828). When the diagnosis of DED was made based on either CNFW or CNBD, the sensitivity was 97.4% and the specificity 46.7%.

Conclusions The software ACCMetrics was able to rapidly detect SNP alterations occurring in the setting of DED and showed good diagnostic performance in discriminating DED patients.

Keywords Dry eye · In vivo confocal microscopy · Sub-basal nerve plexus · Automated analysis · ACCMetrics

Introduction

The human cornea contains sensory nerve fibers that originated from the ophthalmic branch of the trigeminal nerve as well as sympathetic and parasympathetic nerve fibers. Nerve bundles enter the cornea at the periphery, move toward the center below the anterior third of the stroma, and generate a dense network of nerve fibers between Bowman's layer and basal epithelial cells named subbasal nerve plexus (SNP). Corneal nerves play an essential role in the normal metabolism and function of the ocular surface regulating corneal epithelial integrity, proliferation, and wound healing [1]. Neurosensory abnormalities are considered one of the core mechanisms of dry eye disease (DED) and have been recently included in the updated definition of TFOS Dry Eye Workshop (DEWS) II [2].

In vivo confocal microscopy (IVCM) is a non-invasive technique that allows high-resolution visualization of SNP at a cellular level. Previous IVCM studies have documented qualitative/quantitative alterations of corneal nerves' morphology in patients with DED, including decreased nerve density and increased tortuosity, reflectivity, and beading [3–9].

However, despite the use of IVCM in DED clinical practice has gained popularity, there has been no corresponding increase in the availability of software tools to support the

✉ Giuseppe Giannaccare
giannaccare@gmail.com

[1] Ophthalmology Unit, DIMES, S.Orsola-Malpighi University Hospital, University of Bologna, Via Palagi 9, 40138 Bologna, Italy

automated analysis of corneal nerves. In fact, to date, the analysis of corneal nerves detected by IVCM images is mostly based on manual/semiautomated systems, which suffered from several disadvantages, since they are time-consuming, subjective, and prone to observer bias with poor reproducibility and consistency [10]. Indeed, the recent TFOS DEWS II "Pain and Sensation" Subcommittee Report stated that the introduction of methods to automate quantitative IVCM measures would greatly enhance research methodology and interpretation of results [11].

The purpose of this study was to evaluate the morphometric analysis of corneal SNP in DED patients, using newly developed fully automated IVCM software "ACCMetrics," and to further investigate the diagnostic performance of this analysis system in discriminating DED patients from healthy subjects.

Materials and methods

Patients

This cross-sectional study was conducted at a single tertiary-referral center (S.Orsola-Malpighi University Hospital, Bologna, Italy). Patients affected by moderate to severe DED owing to either Sjögren's syndrome (SS) or ocular graft versus host disease (GVHD) were included. Dry eye was ascertained using TFOS DEWS II Criteria [12]. Healthy sex- and age-matched subjects acted as controls. Exclusion criteria for both groups were the use of topical steroids and antibiotics within 2 weeks before analysis, contact lens wearing, previous corneal surgery, history of Stevens–Johnson syndrome, mucous membrane pemphigoid or herpetic keratitis, active ocular allergies, and diabetes. The study was performed in accordance with the principles of the Declaration of Helsinki and was approved by the local Institutional Review Board. Written informed consent was obtained from all subjects included in the study before any procedure.

Ocular surface workup

Ocular surface workup included slit-lamp examination, and measurement of corneal sensitivity, Schirmer test (ST) type I, tear film break-up time (TFBUT), and conjunctival and corneal staining. Briefly, corneal sensitivity was measured in the central cornea using Cochet-Bonnet esthesiometer (Luneau Chartres, France), and recorded in millimeters per nylon filament length. The ST and TFBUT measurements were performed according to the DEWS II guidelines [12]. Corneal and conjunctival staining scores were graded according to the National Eye Institute and van Bijsterveld scales, respectively [13, 14]. Subjective symptoms of ocular discomfort were evaluated using the Ocular Surface Disease Index questionnaire [15]. A 100-mm horizontal Visual Analogue Scale was used to further measure the intensity of symptoms [16].

In vivo confocal microscopy

In vivo confocal microscopy was performed using Heidelberg Retina Tomograph with the Rostock Cornea Module (HRT/RCM, Heidelberg Engineering, Heidelberg, Germany), as previously described [17]. Digital images were recorded with the sequence mode at a rate of three frames per second, including 100 images per sequence. A total of six to eight sequence scans of non-overlapping areas were recorded focusing on the SNP layer, typically at a depth of 50 to 80 μm. All IVCM exams were performed by a single experienced examiner (GG). Three most representative images of corneal subbasal nerves were selected based on technical quality by a masked observer (MP).

Image analysis

Images of corneal SNP were analyzed with "ACCMetrics" (MA Dabbah, Imaging Science and Biomedical Engineering, Manchester, UK), which is a fully automated image analysis software, which employs a machine-learning method [18–20].

The following seven parameters were calculated: (1) corneal nerve fiber density (CNFD), the total number of nerves/mm^2; (2) corneal nerve branch density (CNBD), the number of branches emanating from major nerve trunks/mm^2; (3) corneal nerve fiber length (CNFL), the total length of all nerve fibers and branches (mm/mm^2); (4) corneal nerve total branch density (CTBD), the total number of branches/mm^2; (5) corneal nerve fiber area (CNFA), the total nerve fiber area (mm^2/mm^2); (6) corneal nerve fiber width (CNFW), the average nerve fiber width (mm/mm^2); (7) corneal nerve fractal dimension (CNFrD), a measure of the structural complexity of corneal nerves [21].

The image analysis was applied to each of the three selected images. The average of the three values obtained for each parameter was used for statistical analysis.

Statistical analysis

The SPSS statistical software (SPSS Inc., Chicago, Illinois, USA) was used for data analysis. Values are expressed as mean ± standard deviation (SD). The Mann–Whitney U test was used to compare continuous variables between DED patients and control subjects and between DED patients with SS and ocular GVHD. Receiver operating characteristic (ROC) curves with calculations of the area under the curve (AUC) were used to describe the accuracy of each IVCM parameter for discriminating patients with DED from controls. Sensitivity and specificity

of each parameter were determined for the cutoff value whose corresponding point on the ROC curve was nearest to the coordinate (0,100). A Venn diagram analysis was performed to show how the combinations of IVCM parameters were able to discriminate patients with DED from controls. A p value < 0.05 was considered statistically significant.

Results

A total of 39 patients with DED were included in the study (14 males and 25 females; mean age 64.3 ± 14.5 years). Of these, 20 patients had SS, while 19 patients had ocular GVHD. Thirty healthy subjects were included as a control group (12 males and 18 females; mean age 66.1 ± 10.2 years). No significant differences were found for age and sex between DED patients and control subjects (always $p > 0.05$). Ocular surface parameters of DED patients and control subjects are summarized in Table 1. Representative IVCM images analyzed with ACCMetrics from one control subject and one patient with DED are shown in Fig. 1a–d).

The values of each IVCM parameter obtained with the software ACCMetrics in the two groups are reported in Table 2. Significantly, lower values of CNFD, CNBD, and CNFL were found in DED patients compared to controls (respectively, 20.5 ± 8.7 vs 25.4 ± 6.7 n/mm^2, $p = 0.008$; 25.6 ± 20.1 vs 37.6 ± 21.5 n/mm^2, $p = 0.010$; 12.6 ± 4.4 vs 14.5 ± 2.9 mm/mm^2, $p = 0.024$). Conversely, CNFW value was significantly higher in DED patients compared to controls (0.021 ± 0.001 vs 0.019 ± 0.001 mm/mm^2; $p < 0.001$). The values of IVCM metrics were then analyzed separately according to the underlying disease (namely SS and ocular GVHD). No significant differences were found in any of the IVCM parameters in the two subgroups of DED patients (Table 3).

Table 4 shows the AUC values of ROC curves with 95% confidence intervals, sensitivity, and specificity of IVCM parameters for discriminating DED patients from healthy subjects. The AUC values showed that CNFW had the highest diagnostic power (0.828), followed by CNBD (0.698), CNFD (0.686), CNFL (0.660), CTBD (0.626), CNFrD (0.606), and CNFA (0.585).

The ROC curves of the four parameters with a value of AUC significantly higher than 0.5 (CNFW, CNBD, CNFD, and CNFL; always $p < 0.05$) are shown in Fig. 2. The cutoff values of these four parameters to diagnose DED were as follows: CNFW > 0.02, CNBD ≤ 29.2, CNFD ≤ 22.9 and CNFL ≤ 14.0. A Venn diagram analysis was performed to show how these four parameters were able to discriminate patients with DED from controls (Fig. 3).

The two parameters with the highest AUC (namely CNFW and CNBD) were combined in parallel, and the diagnostic accuracy was calculated. When the diagnosis of DED was made based on either CNFW or CNBD being abnormal, the sensitivity was 97.4% and the specificity was 46.7%; when the diagnosis was made on both CNFW and CNBD being abnormal, the sensitivity was 66.7% and the specificity was 90.0%.

Discussion

Valid and reliable quantification of the structural status of the SNP is fundamental to optimize detection, monitor progression, and assess the efficacy of treatment strategies in ocular surface disease. In the present study, we used a newly developed automated system "ACCMetrics" for analyzing corneal SNP in both DED patients and control subjects, and then we calculated the diagnostic performance of this system for reaching the diagnosis of DED. This image analysis system was originally introduced and validated in the setting of diabetic corneal neuropathy, while poor information are available regarding morphometric analysis and diagnostic performance in DED patients [22]. Our results showed that patients with DED had a lower density of nerve fibers and branches and shorter nerve fibers. Poor consistency has been shown in the literature regarding the

Table 1 Ocular surface parameters in patients with DED and in control subjects

Parameter	DED patients (mean ± SD)	Control subjects (mean ± SD)	*P*
OSDI (score)	50.8 ± 18.8	7.3 ± 3.1	*< 0.001*
VAS (score)	6.8 ± 1.5	1.0 ± 0.8	*< 0.001*
Schirmer test (mm/5′)	7.1 ± 6.0	24.3 ± 10.8	*< 0.001*
TFBUT (seconds)	3.7 ± 2.5	10.4 ± 3.6	*< 0.001*
Corneal staining (NEI score)	6.4 ± 2.7	0.6 ± 0.8	*< 0.001*
Conjunctival staining (VB score)	7.3 ± 2.9	0.9 ± 0.9	*< 0.001*
Corneal sensitivity (mm)	52.3 ± 2.1	54.5 ± 1.6	*< 0.001*

Statistically significant p values are reported in italics

DED, dry eye disease; *OSDI*, ocular surface disease index; *VAS*, visual analogue scale; *TFBUT*, tear film break-up time; *NEI* National Eye Institute; *VB*, van Bijsterveld; *SD*, standard deviation

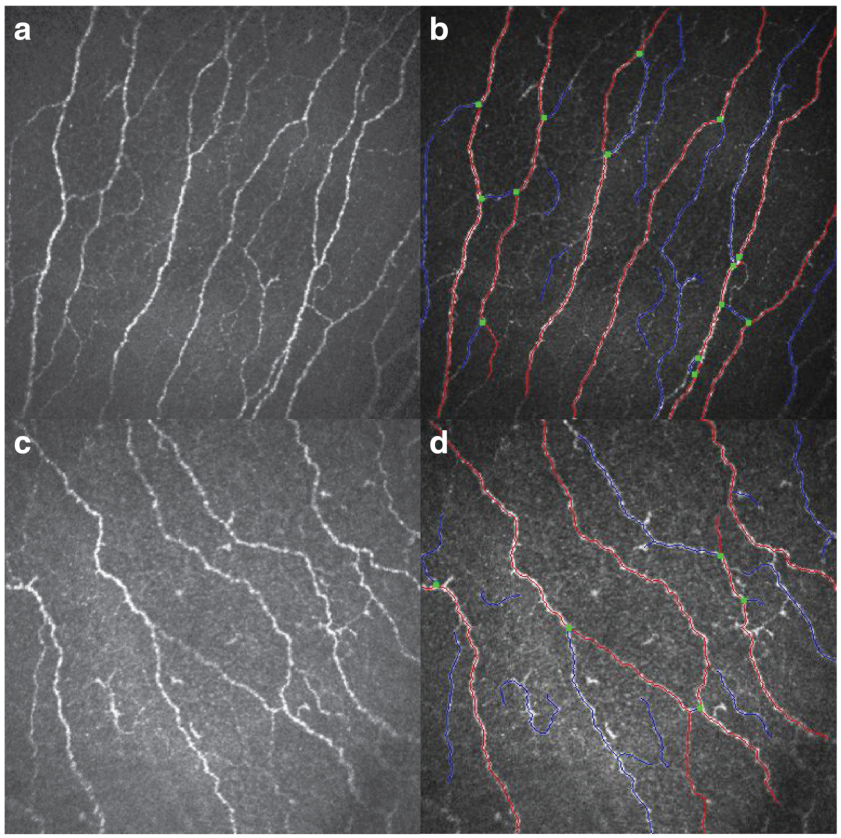

Fig. 1 **a** Representative IVCM images from one control subject and **c** one patient with dry eye disease. **b** Automated image analysis using ACCMetrics software of the same control subject and **d** dry eye disease patient. Main nerve fibers are indicated in red, nerve branches in blue, and branch points in green

changes in nerve density in DED patients. In fact, while the majority of the available studies have reported a decrease of density [5, 7, 8] in agreement with our findings, other studies observed no change [3], or even an increase of density in DED patients [6]. These discrepancies have been attributed to either different types, stages, and severities of DED populations under study that may induce different degeneration/regeneration patterns of corneal nerves [11].

Interestingly, we found that patients with DED had an increased corneal nerve fiber width compared to controls. The ROC analysis showed that the parameter CNFW had the highest AUC (0.820), and, therefore, it has the highest power to discriminate between DED patients and control subjects. An increased nerve fiber width was reported in patients with DED only in a previous study employing a semiautomated analysis system [8]. This morphological alteration is thought

Table 2 In vivo confocal microscopy automated morphometric analysis of corneal subbasal nerve plexus in patients with DED ($n = 39$) and in control subjects ($n = 30$)

Parameter	DED patients (mean ± SD)	Control subjects (mean ± SD)	*p*
CNFD (n/mm^2)	20.5 ± 8.7	25.4 ± 6.7	*0.008*
CNBD (n/mm^2)	25.6 ± 20.1	37.6 ± 21.5	*0.010*
CNFL (mm/mm^2)	12.6 ± 4.4	14.5 ± 2.9	*0.024*
CTBD (n/mm^2)	42.3 ± 30.0	55.8 ± 33.5	0.075
CNFA (mm^2/mm^2)	0.006 ± 0.002	0.006 ± 0.003	0.228
CNFW (mm/mm^2)	0.021 ± 0.001	0.019 ± 0.001	*< 0.001*
CNFrD	1.47 ± 0.04	1.48 ± 0.02	0.135

Statistically significant *p* values are reported in italics

DED, dry eye disease; *CNFD*, corneal nerve fiber density; *CNBD*, corneal nerve branch density; *CNFL*, corneal nerve fiber length; *CTBD*, corneal nerve total branch density; *CNFA*, corneal nerve fiber area; *CNFW* corneal nerve fiber width; *CNFrD*, corneal nerve fractal nerve density

Table 3 In vivo confocal microscopy automated morphometric analysis of corneal subbasal nerve plexus in patients with Sjögren's syndrome ($n = 20$) and ocular GVHD ($n = 19$)

Parameter	Sjögren's syndrome	Ocular GVHD	*P*
CNFD	21.1 ± 5.9	19.7 ± 11.0	0.290
CNBD	23.1 ± 15.4	28.6 ± 24.8	0.842
CNFL	13.0 ± 3.5	12.3 ± 5.2	0.286
CTBD	40.7 ± 22.6	44.1 ± 33.3	0.844
CNFA	0.006 ± 0.002	0.006 ± 0.003	0.768
CNFW	0.021 ± 0.001	0.022 ± 0.002	0.527
CNFrD	1.48 ± 0.03	1.46 ± 0.05	0.177

CNFD, corneal nerve fiber density; *CNBD*, corneal nerve branch density; *CNFL*, corneal nerve fiber length; *CTBD*, corneal nerve total branch density; *CNFA*, corneal nerve fiber area; *CNFW* corneal nerve fiber width; *CNFrD*, corneal nerve fractal nerve density

Table 4 Areas under the curves (AUC) with 95% confidence intervals (CIs), sensitivity, and specificity of each in vivo confocal microscopy parameter for the discrimination between DED patients and control subjects. Sensitivity and specificity were determined at the cutoff value whose corresponding point on the ROC curve was nearest to the coordinate (0,100)

Parameter	AUC	95% CIs	Criterion	Sensitivity (%)	Specificity (%)
CNFW	0.828	0.718 to 0.908	> 0.0198 mm/mm^2	89.7	70.0
CNBD	0.698	0.576 to 0.803	≤ 29.17 n/mm^2	74.4	66.7
CNFD	0.686	0.563 to 0.792	≤ 22.92 n/mm^2	71.8	66.7
CNFL	0.660	0.536 to 0.770	≤ 13.96 mm/mm^2	66.7	60.0
CTBD	0.626	0.501 to 0.739	≤ 35.41 n/mm^2	53.8	73.3
CNFrD	0.606	0.481 to 0.721	≤ 1.476	59.0	66.7
CNFA	0.585	0.460 to 0.702	≤ 0.0055 mm^2/mm^2	53.8	63.3

DED, dry eye disease; *CNFW*, corneal nerve fiber width; *CNBD*, corneal nerve branch density; *CNFD*, corneal nerve fiber density; *CNFL*, corneal nerve fiber length; *CTBD*, corneal nerve total branch density; *CNFrD*, corneal nerve fractal nerve density; *CNFA*, corneal nerve fiber area

to be caused by the loss of smaller nerve fibers with the preservation of thicker bundles, a microstructural change that was demonstrated also in other small fiber diseases, such as diabetic or sarcoidosis-associated neuropathy [23, 24]. In addition to the nerve fiber drop out, the chronic inflammation occurring in DED could cause nerve fiber swelling or stimulate the release of neurotrophic factors, which are known to induce peripheral nerves hypertrophy [8, 25].

Corneal nerve fractal dimension is a novel IVCM parameter obtained with the introduction of the updated version of ACCMetrics. This metric measures the structural complexity of corneal nerves and may provide an additional means of differentiating patients with neuropathies of different etiologies [21]. In previous work, CNFrD demonstrated a diagnostic efficiency comparable to conventional IVCM parameters in identifying patients with diabetic neuropathy [21]. We

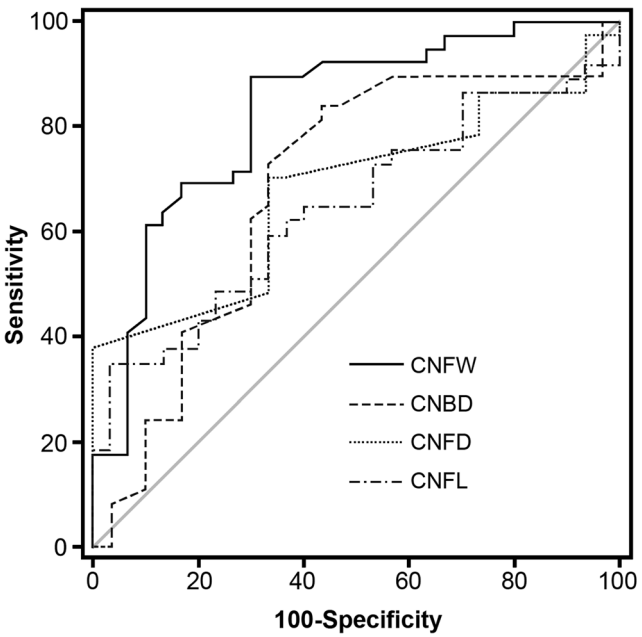

Fig. 2 Receiver operating characteristic curves for corneal nerve fiber width (CNFW), corneal nerve branch density (CNBD), corneal nerve fiber density (CNFD), and corneal nerve fiber length (CNFL)

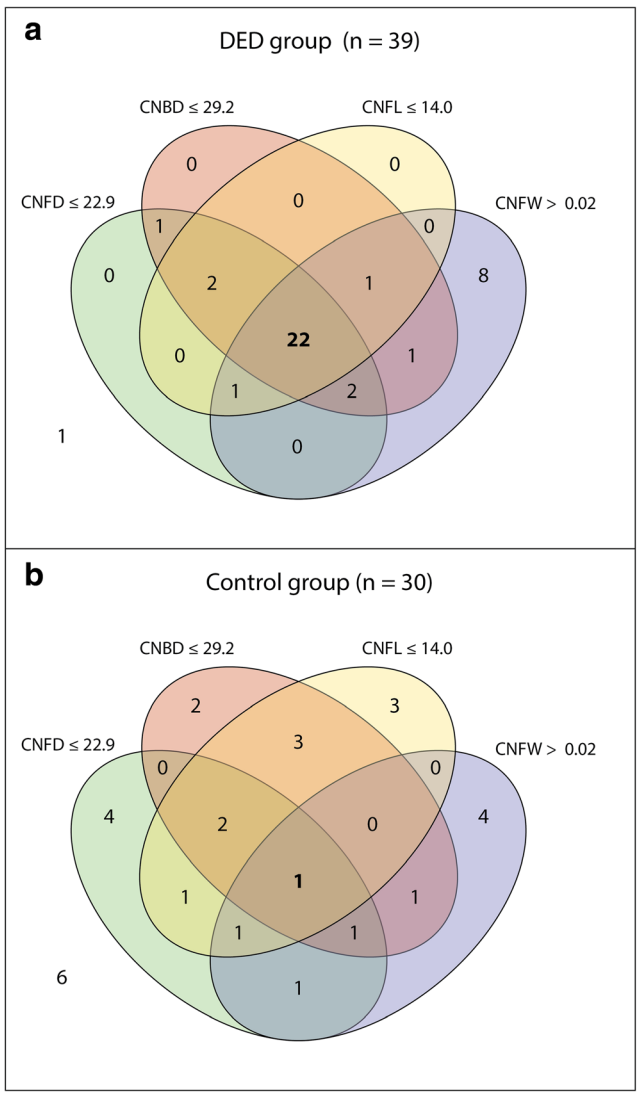

Fig. 3 Venn diagram analysis of **a** dry eye disease (DED) group and **b** control group. Cutoff values of corneal nerve fiber density (CNFD), corneal nerve branch density (CNBD), corneal nerve fiber length (CNFL), and corneal nerve fiber width (CNFW) were determined from the receiver operating characteristic curves

measured for the first time CNFrD in patients with DED and compared these values with the ones obtained from control subjects. This parameter did not show any significant difference between the two groups, with a lower diagnostic power compared to the other conventional IVCM parameters.

In this study, the parameters CNFW and CNBD resulted as the tests with the highest diagnostic power; by combining the two tests in parallel, DED may be strongly suspected when at least one of these two tests is abnormal.

It has been previously demonstrated that patients with DED owing to underlying systemic immune diseases (SS and GVHD) exhibit higher density, size, and a number of dendritic cells compared to those with DED of non-immune etiology [17]. In addition, a decreased density of nerves in the SNP, as well as a greater number of beaded nerves, were found in both non-SS and SS DED patients compared to controls [5]. Conversely, no significant differences in morphologic IVCM parameters have been detected comparing GVHD and SS patients [17, 26]. To elucidate this point, we conducted a further sub-analysis that compared IVCM metrics in these two groups, which did not identify any significant difference, in agreement with the abovementioned studies. We hypothesize that ocular surface cellular changes observed by IVCM may be possibly reflective of the local disease severity rather than the underlying systemic process.

Our study suffers from several limitations, concerning both the study design and the technical aspects of the software used. Firstly, our sample size was small and included patients with SS and ocular GVHD referred to a tertiary center; therefore, corneal nerve alterations may be less common or pronounced in DED population with milder stages of the disease. Larger datasets over a broad range of DED severity and type are required to validate these preliminary results in this setting. Secondly, ACCMetrics does not analyze and quantify nerve tortuosity, a well-recognized IVCM metric affected in DED. Thus, the diagnostic performance of this analysis system in the setting of dry eye disease could be further improved by also incorporating this parameter among the evaluated metrics, as already available in the manual version of the software "CCMetrics" [23]. Additionally, despite a previous study showing that automated quantification of SNP provided comparable ability to manual and semiautomated methods in detecting corneal neuropathy [27], both false-negative and false-positive errors are possible, and include respectively the failure to detect thin nerves (Fig. 1b), and the erroneous recognition of other structures such as dendritic cells (Fig. 1d). However, ACCMetrics is about 7× and 4× faster than the manual semiautomated and automated morphometric methods respectively [27], and thus its application may be particularly helpful for large trials that require analysis of high numbers of IVCM images.

In conclusion, the present study represents the first application of ACCMetrics as a novel tool for the rapid, automated, and quantitative morphometric analysis of SNP alterations occurring in the setting of dry eye disease. The values of CNFD, CNBD, and CNFL were lower, while the value of CNFW was higher in DED patients compared to controls. Additionally, ACCMetrics showed a good diagnostic performance in discriminating DED patients from control subjects, with CNFW and CNBD being the two parameters with the highest diagnostic power.

Acknowledgments We thank Prof. Rayaz Malik and Collaborators from the University of Manchester (UK) for their kind permission to use the "ACCMetrics" software for the automated analysis of the in vivo confocal microscopy images in the present work.

Compliance with ethical standards

Conflict of interest The authors declare that they have no conflict of interest.

Ethical approval All procedures performed in studies involving human participants were in accordance with the ethical standards of the institutional and/or national research committee and with the 1964 Helsinki declaration and its later amendments or comparable ethical standards.

Informed consent Informed consent was obtained from all individual participants included in the study.

Publisher's Note Springer Nature remains neutral with regard to jurisdictional claims inpublished maps and institutional affiliations.

References

1. Muller LJ, Marfurt CF, Kruse F, Tervo TM (2003) Corneal nerves: structure, contents and function. Exp Eye Res 76:521–542
2. Craig JP, Nichols KK, Akpek EK, Caffery B, Dua HS, Joo CK et al (2017) TFOS DEWS II definition and classification report. Ocul Surf 15:276–283. https://doi.org/10.1016/j.jtos.2017.05.008
3. Tuominen IS, Konttinen YT, Vesaluoma MH, Moilanen JA, Helintö M, Tervo TM (2003) Corneal innervation and morphology in primary Sjögren's syndrome. Invest Ophthalmol Vis Sci 44: 2545–2549
4. Zhang M, Chen J, Luo L, Xiao Q, Sun M, Liu Z (2005) Altered corneal nerves in aqueous tear deficiency viewed by in vivo confocal microscopy. Cornea 24:818–824
5. Benítez del Castillo JM, Wasfy MA, Fernandez C, Garcia-Sanchez J (2004) An in vivo confocal masked study on corneal epithelium and subbasal nerves in patients with dry eye. Invest Ophthalmol Vis Sci 45:3030–3035
6. Hoşal BM, Ornek N, Zilelioğlu G, Elhan AH (2005) Morphology of corneal nerves and corneal sensation in dry eye: a preliminary study. Eye (Lond) 19:1276–1279
7. Villani E, Galimberti D, Viola F, Mapelli C, Ratiglia R (2007) The cornea in Sjogren's syndrome: an in vivo confocal study. Invest Ophthalmol Vis Sci 48:2017–2022
8. Labbé A, Liang Q, Wang Z, Zhang Y, Xu L, Baudouin C et al (2013) Corneal nerve structure and function in patients with non-

Sjogren dry eye: clinical correlations. Invest Ophthalmol Vis Sci 54:5144–5150. https://doi.org/10.1167/iovs.13-12370

9. Giannaccare G, Buzzi M, Fresina M, Velati C, Versura P (2017) Efficacy of 2-month treatment with cord blood serum eye drops in ocular surface disease: an in vivo confocal microscopy study. Cornea 36:915–921. https://doi.org/10.1097/ICO.0000000000001257
10. Petropoulos IN, Manzoor T, Morgan P, Fadavi H, Asghar O, Alam U et al (2013) Repeatability of in vivo corneal confocal microscopy to quantify corneal nerve morphology. Cornea 32:e83–e89. https://doi.org/10.1097/ICO.0b013e3182749419
11. Belmonte C, Nichols JJ, Cox SM, Brock JA, Begley CG, Bereiter DA et al (2017) TFOS DEWS II pain and sensation report. Ocul Surf 15:404–437. https://doi.org/10.1016/j.jtos.2017.05.002
12. Wolffsohn JS, Arita R, Chalmers R, Djalilian A, Dogru M, Dumbleton K et al (2017) TFOS DEWS II diagnostic methodology report. Ocul Surf 15:539–574. https://doi.org/10.1016/j.jtos.2017.05.001
13. Lemp MA (1995) Report of the National Eye Institute/Industry Workshop on clinical trials in dry eye. CLAO J 21:221–232
14. Van Bijsterveld OP (1969) Diagnostic tests in the sicca syndrome. Arch Ophthalmol 82:10–14
15. Schiffman RM, Christianson MD, Jacobsen G, Hirsch JD, Reis BL (2000) Reliability and validity of the ocular surface disease index. Arch Ophthalmol 118:615–621
16. Jensen MP, Karoly P, Braver S (1986) The measurement of clinical pain intensity: a comparison of six methods. Pain 27:117–126
17. Kheirkhah A, Rahimi Darabad R, Cruzat A, Hajrasouliha AR, Witkin D, Wong N et al (2015) Corneal epithelial immune dendritic cell alterations in subtypes of dry eye disease: a pilot in vivo confocal microscopic study. Invest Ophthalmol Vis Sci 56:7179–7185. https://doi.org/10.1167/iovs.15-17433
18. Dabbah MA, Graham J, Petropoulos IN, Tavakoli M, Malik RA (2011) Automatic analysis of diabetic peripheral neuropathy using multi-scale quantitative morphology of nerve fibres in corneal confocal microscopy imaging. Med Image Anal 15:738–747. https://doi.org/10.1016/j.media.2011.05.016
19. Dabbah MA, Graham J, Petropoulos I, Tavakoli M, Malik RA (2010) Dual-model automatic detection of nerve-fibres in corneal confocal microscopy images. Med Image Comput Comput Assist Interv 13:300–307
20. Chen X, Graham J, Dabbah MA, Petropoulos IN, Tavakoli M, Malik RA (2017) An automatic tool for quantification of nerve fibers in corneal confocal microscopy images. IEEE Trans Biomed Eng 64:786–794. https://doi.org/10.1109/TBME.2016.2573642
21. Chen X, Graham J, Petropoulos IN, Ponirakis G, Asghar O, Alam U et al (2018) Corneal nerve fractal dimension: a novel corneal nerve metric for the diagnosis of diabetic sensorimotor polyneuropathy. Invest Ophthalmol Vis Sci 59:1113–1118. https://doi.org/10.1167/iovs.17-23342
22. Shetty R, Sethu S, Deshmukh R, Deshpande K, Ghosh A, Agrawal A et al (2016) Corneal dendritic cell density is associated with subbasal nerve plexus features, ocular surface disease index, and serum vitamin D in evaporative dry eye disease. Biomed Res Int 2016:4369750. https://doi.org/10.1155/2016/4369750
23. Szalai E, Deak E, Modis L Jr, Németh G, Berta A, Nagy A et al (2016) Early corneal cellular and nerve fiber pathology in young patients with type 1 diabetes mellitus identified using corneal confocal microscopy. Invest Ophthalmol Vis Sci 57:853–8588. https://doi.org/10.1167/iovs.15-18735
24. Brines M, Culver DA, Ferdousi M, Tannemaat MR, van Velzen M, Dahan A et al (2018) Corneal nerve fiber size adds utility to the diagnosis and assessment of therapeutic response in patients with small fiber neuropathy. Sci Rep 8:4734. https://doi.org/10.1038/s41598-018-23107-w
25. Belmonte C, Acosta MC, Gallar J (2004) Neural basis of sensation in intact and injured corneas. Exp Eye Res 78:513–525
26. Tepelus TC, Chiu GB, Maram J, Huang J, Chopra V, Sadda SR et al (2017) Corneal features in ocular graft-versus-host disease by in vivo confocal microscopy. Graefes Arch Clin Exp Ophthalmol 255:2389–2397. https://doi.org/10.1007/s00417-017-3759-x
27. Dehghani C, Pritchard N, Edwards K, Russell AW, Malik RA, Efron N (2014) Fully automated, semiautomated, and manual morphometric analysis of corneal subbasal nerve plexus in individuals with and without diabetes. Cornea 33:696–702